

# A Novel Star-Shaped Zinc Porphyrin Cored [5]Rotaxane

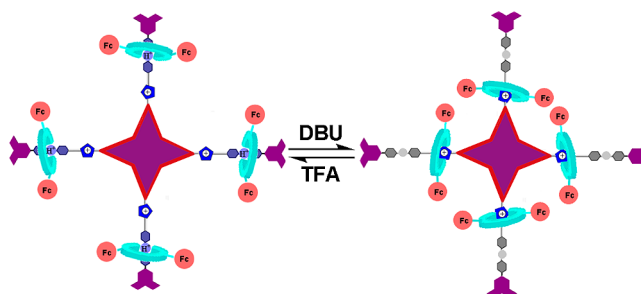
Hui Zhang, Qiang Liu, Jing Li, and Da-Hui Qu\*

Key Laboratory for Advanced Materials and Institute of Fine Chemicals, East China University of Science & Technology, Shanghai 200237, P. R. China

dahui\_qu@ecust.edu.cn

Received November 28, 2012

## ABSTRACT



A novel star-shaped zinc porphyrin cored [5]rotaxane with four rotaxane arms was synthesized and well characterized by  $^1\text{H}$ ,  $^{13}\text{C}$  NMR spectroscopy and HR-ESI mass spectrometry. The introduction of the zinc porphyrin core enabled the [5]rotaxane to have a fixed shape and symmetrical structure, and the simultaneous shuttling motion of four macrocycles can be driven by external acid–base stimuli. This kind of topological structure exhibits important potential in the design and construction of large sophisticated assemblies.

With the development of topological chemistry and dynamic covalent chemistry, more and more sophisticated mechanically interlocked compounds with complicated structures and highly symmetrical shapes, such as rotaxanes,<sup>1</sup> catenanes,<sup>2</sup> molecular elevators,<sup>3</sup> Borromean rings,<sup>4</sup> Solomon's knots,<sup>5</sup> trefoil knots,<sup>6</sup> and molecular necklaces,<sup>7</sup> have been reported. In all reported mechanically

interlocked molecules, rotaxanes have been extensively and thoroughly investigated because of their excellent properties and convenient syntheses. However, the synthesis of highly ordered or symmetrical [n]rotaxane with predetermined shapes still remains a challenge for chemists because of the synthetic difficulty.<sup>8</sup> As we know, the geometry of the

(1) (a) Raymo, F. M.; Stoddart, J. F. *Chem. Rev.* **1999**, *99*, 1643–1663. (b) Balzani, V.; Credi, A.; Silvi, S.; Venturi, M. *Chem. Soc. Rev.* **2006**, *35*, 1135–1149. (c) Tian, H.; Wang, Q.-C. *Chem. Soc. Rev.* **2006**, *35*, 361–374. (d) Saha, S.; Stoddart, J. F. *Chem. Soc. Rev.* **2007**, *36*, 77–92. (e) Champin, B.; Mobian, P.; Sauvage, J.-P. *Chem. Soc. Rev.* **2007**, *36*, 358–366. (f) Crowley, J. D.; Goldup, S. M.; Lee, A.-L.; Leigh, D. A.; McBurney, R. T. *Chem. Soc. Rev.* **2009**, *38*, 1530–1541. (g) Hänni, K. D.; Leigh, D. A. *Chem. Soc. Rev.* **2010**, *39*, 1240–1251. (h) Mateo-Alonso, A. *Chem. Commun.* **2010**, 9089–9099. (i) Zhu, L.-L.; Yan, H.; Nguyen, K. T.; Tian, H.; Zhao, Y.-L. *Chem. Commun.* **2012**, 4290–4292. (j) Zhu, L.-L.; Yan, H.; Wang, X.-J.; Zhao, Y.-L. *J. Org. Chem.* **2012**, *77*, 10168–10175.

(2) (a) Payer, D.; Rauschenbach, S.; Malinowski, N.; Konuma, M.; Virojanadara, C.; Starke, U.; Dietrich-Buchecker, C.; Collin, J. P.; Sauvage, J.-P.; Lin, N.; Kern, K. *J. Am. Chem. Soc.* **2007**, *129*, 15662–15667. (b) Liu, M.; Li, S.-J.; Hu, M.-L.; Wang, F.; Huang, F.-H. *Org. Lett.* **2010**, *12*, 760–763. (c) Fang, L.; Wang, C.; Fahrenbach, A. C.; Trabolsi, A.; Botros, Y. Y.; Stoddart, J. F. *Angew. Chem., Int. Ed.* **2011**, *50*, 1805–1809.

(3) (a) Badjić, J. D.; Balzani, V.; Credi, A.; Silvi, S.; Stoddart, J. F. *Science* **2004**, *303*, 1845–1849. (b) Badjić, J. D.; Ronconi, C. M.; Stoddart, J. F.; Balzani, V.; Silvi, S.; Credi, A. *J. Am. Chem. Soc.* **2006**, *128*, 1489–1499.

(4) (a) Chichak, K. S.; Cantrill, S. J.; Pease, A. R.; Chiu, S.-H.; Cave, G. W. V.; Atwood, J. L.; Stoddart, J. F. *Science* **2004**, *304*, 1308–1312. (b) Meyer, C. D.; Forgan, R. S.; Chichak, K. S.; Peters, A. J.; Tangchaivang, N.; Cave, G. W. V.; Khan, S. I.; Cantrill, S. J.; Stoddart, J. F. *Chem.—Eur. J.* **2010**, *16*, 12570–12581.

(5) (a) Niergarten, J.-F.; Dietrich-Buchecker, C. O.; Sauvage, J.-P. *J. Am. Chem. Soc.* **1994**, *116*, 375–376. (b) Ibukuro, F.; Fujita, M.; Yamaguchi, K.; Sauvage, J.-P. *J. Am. Chem. Soc.* **1999**, *121*, 11014–11015. (c) Pentecost, C. D.; Chichak, K. S.; Peters, A. J.; Cave, G. W. V.; Cantrill, S. J.; Stoddart, J. F. *Angew. Chem., Int. Ed.* **2007**, *46*, 218–222.

(6) (a) Dietrich-Buchecker, C. O.; Sauvage, J.-P. *Angew. Chem., Int. Ed.* **1989**, *28*, 189–192. (b) Dietrich-Buchecker, C. O.; Niergarten, J. F.; Sauvage, J.-P.; Armaroli, N.; Balzani, V.; De Cola, L. *J. Am. Chem. Soc.* **1993**, *115*, 11234–11237. (c) Dietrich-Buchecker, C. O.; Rapenne, G.; Sauvage, J.-P. *Chem. Commun.* **1997**, 2053–2054. (d) Dirk, A. *New J. Chem.* **2006**, *30*, 873–882.

(7) (a) Roh, S.-G.; Park, K.-M.; Park, G.-J.; Sakamoto, S.; Yamaguchi, K.; Kim, K. *Angew. Chem., Int. Ed.* **1999**, *38*, 637–641. (b) Kim, K. *Chem. Soc. Rev.* **2002**, *31*, 96–107. (c) Chang, C.-F.; Chuang, C.-J.; Lai, C.-C.; Liu, Y.-H.; Peng, S.-M.; Chiu, S.-H. *Angew. Chem., Int. Ed.* **2012**, *51*, 10094–10098.

(8) (a) Bonnet, S.; Collin, J.-P.; Koizumi, M.; Mobian, P.; Sauvage, J.-P. *Adv. Mater.* **2006**, *18*, 1239–1250. (b) Zhang, Z.-J.; Zhang, H.-Y.; Wang, H.; Liu, Y. *Angew. Chem., Int. Ed.* **2011**, *50*, 10834–10838.

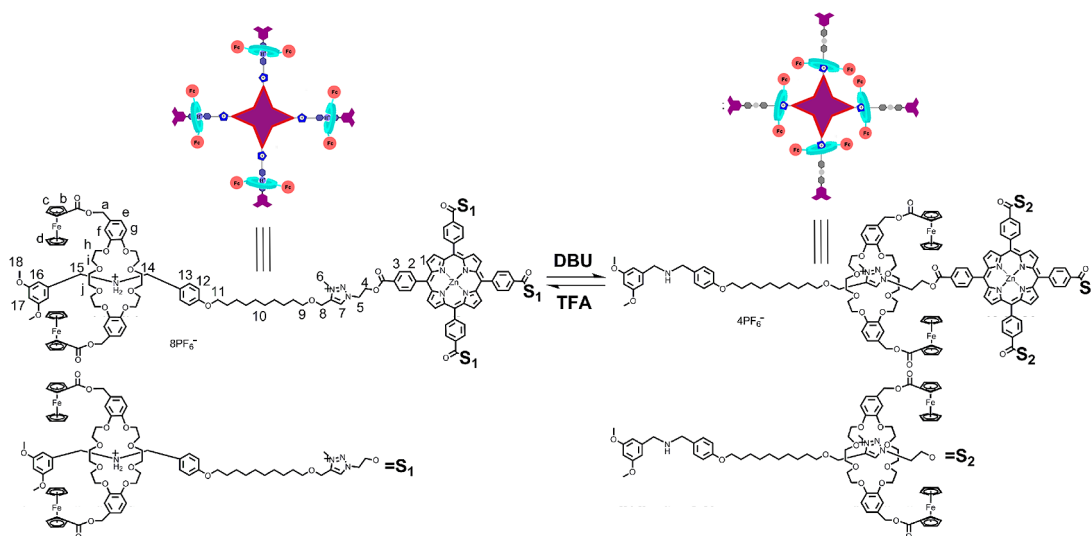


**Figure 1.** Chemical structure and schematic presentation of target star-shaped zinc porphyrin cored [5]rotaxane **1-H**.

rotaxane is determined by the topology of the individual components. It can be concluded that the utilization of molecular building blocks with invariable and unambiguous shapes and exclusive reaction sites can lead to the formation of rotaxanes with fixed shapes. This fact inspired us to find molecular building blocks with symmetrical shapes and synthesize a highly symmetrical [*n*]rotaxane.

In this paper, we report the design, synthesis, characterization, and shuttling motion of a star-shaped zinc porphyrin cored [5]rotaxane, in which each of the four substituted dibenzo-24-crown-8 (DB24C8) macrocycles was interlocked onto a branch of the star-shaped compound with a zinc porphyrin core bearing a rigid structure and symmetrical shape. Porphyrin was selected as the modular building block because of not only its well-defined shape and size but also its convenient modification.<sup>9</sup> In this novel star-shaped zinc porphyrin cored [5]rotaxane, four DB24C8 macrocycles can shuttle between two recognition sites simultaneously under the external acid–base stimuli, which was confirmed using <sup>1</sup>H NMR spectroscopy. This kind of rotaxane will be beneficial for the construction of more sophisticated mechanically interlocked molecules.

The syntheses, molecular structures, and schematic representations of [5]rotaxane **1-H**, **2-H**, and the reference compound ferrocene-containing crown ether **5** are shown in Figures 1 and 2. The target star-shaped zinc porphyrin cored [5]rotaxane **1-H** contains four DB24C8 macrocycles, each of which encircles the thread of the [5]rotaxane bearing a zinc porphyrin core with a rigid structure and symmetrical shape. There are two distinguishable binding

sites for DB24C8, namely, dibenzylammonium (DBA)<sup>10</sup> and *N*-methyltriazolium (MTA)<sup>11</sup> recognition sites. The *N*-methyltriazolium (MTA) moiety was used as a less favorable recognition site for DB24C8 upon deprotonation of a more favorable R<sub>2</sub>NH<sup>2+</sup> binding site, and a long-distance alkyl chain was introduced to the thread skeleton to separate the two distinguishable binding sites. Deprotonation with a base can drive the macrocycles to reside in the MTA stations, and it should be noted that the shuttling movement of macrocycles between stations on the thread is simultaneous.

The structure of alkyne **3**, incorporating a DBA unit as a primary recognition site for DB24C8 in the middle, terminated at one end by a 3,5-dimethoxy benzene stopper, and at the other end by a terminal alkyne group, is shown in Figure 2. The syntheses of alkyne **3** and the key macrocycle, crown ether **5**, were reported in our previous work.<sup>12</sup> The key intermediate azide **4** has a zinc porphyrin core and four azide functional groups at each end, which was synthesized starting from compound **P-1**.<sup>13</sup> The ester was hydrolyzed in a 10% NaOH solution (CH<sub>3</sub>CH<sub>2</sub>OH/

(9) (a) Harriman, A.; Sauvage, J.-P. *Chem. Soc. Rev.* **1996**, *26*, 41–48. (b) Li, Y.; Cao, L.-F.; Tian, H. *J. Org. Chem.* **2006**, *71*, 8279–8282. (c) Saha, S.; Flood, A. H.; Stoddart, J. F.; Impellizzeri, S.; Silvi, S.; Venturi, M.; Credi, A. *J. Am. Chem. Soc.* **2007**, *129*, 12159–12171. (d) Liu, Y.; Ke, C.-F.; Zhang, H.-Y.; Cui, J.; Ding, F. *J. Am. Chem. Soc.* **2008**, *130*, 600–605. (e) Wang, K.-R.; Guo, D.-S.; Jiang, B.-P.; Liu, Y. *Chem. Commun.* **2012**, 3644–3646.

(10) (a) Ashton, P. R.; Baxter, I. W.; Raymo, F. M.; Stoddart, J. F.; White, A. J. P.; Williams, D. J.; Wolf, R. *Angew. Chem., Int. Ed.* **1998**, *37*, 1913–1916. (b) Zhang, C.-J.; Li, S.-J.; Zhang, J.-Q.; Zhu, K.-L.; Li, N.; Huang, F.-H. *Org. Lett.* **2007**, *9*, 5553–5556. (c) Zhou, W.-D.; Li, J.-B.; He, X.-R.; Li, C.-H.; Lv, J.; Li, Y.-L.; Wang, S.; Liu, H.-B.; Zhu, D.-B. *Chem.—Eur. J.* **2008**, *14*, 754–763. (d) Jiang, Q.; Zhang, H.-Y.; Han, M.; Ding, Z.-J.; Liu, Y. *Org. Lett.* **2010**, *12*, 1728–1731. (e) Qu, D.-H.; Feringa, B. L. *Angew. Chem., Int. Ed.* **2010**, *49*, 1107–1110.

(11) (a) Coutrot, F.; Romuald, C.; Busseron, E. *Org. Lett.* **2008**, *10*, 3741–3744. (b) Coutrot, F.; Busseron, E. *Chem.—Eur. J.* **2008**, *14*, 4784–4787. (c) Romuald, C.; Busseron, E.; Coutrot, F. *J. Org. Chem.* **2010**, *75*, 6516–6531. (d) Busseron, E.; Romuald, C.; Coutrot, F. *Chem.—Eur. J.* **2010**, *16*, 10062–10073.

(12) (a) Zhang, H.; Kou, X.-X.; Zhang, Q.; Qu, D.-H.; Tian, H. *Org. Biomol. Chem.* **2011**, *9*, 4051–4056. (b) Zhang, H.; Hu, J.; Qu, D.-H. *Org. Lett.* **2012**, *14*, 2334–2337. (c) Zhang, H.; Zhou, B.; Li, H.; Qu, D.-H.; Tian, H. *J. Org. Chem.* DOI: 10.1021/jo302107a. (d) Li, H.; Zhang, H.; Zhang, Q.; Zhang, Q.-W.; Qu, D.-H. *Org. Lett.* **2012**, *14*, 5900–5903.

(13) Gianferrara, T.; Bergamo, A.; Bratsos, I.; Milani, B.; Spagnoli, C.; Sava, G.; Alessio, E. *J. Med. Chem.* **2010**, *53*, 4678–4690.

H<sub>2</sub>O = 4/1) to afford compound **P-2**, which was further esterified with 2-bromoethanol under the condition of EDCI and DMAP in CH<sub>2</sub>Cl<sub>2</sub> to obtain compound **P-3**. In order to avoid the nitrogen reactions, we decided to treat the porphyrin core with zinc acetate. After that, the zinc porphyrin compound **P-4** reacted with sodium azide to produce the azide intermediate **4**.

The selective and effective interaction between a dibenzylammonium ion (R<sub>2</sub>NH<sub>2</sub><sup>+</sup>) and a dibenzo-24-crown-8 (DB24C8) ring was chosen as the binding motif in the design of the rotaxane. The widely used “click chemistry”, namely, Cu(I)-catalyzed azide–alkyne cycloaddition,<sup>14</sup> was chosen as the end-capping method in the preparation of rotaxane **2-H** due to its functional group tolerance and high yield. As shown in Figure 2, alkyne **3** and crown ether **5** were mixed in dry CH<sub>2</sub>Cl<sub>2</sub> at room temperature, after which azide **4** and Cu(CH<sub>3</sub>CN)<sub>4</sub>PF<sub>6</sub> as the catalyst were added to the solution, and the mixture was stirred for two days to form the rotaxanes **2-H** in a 50% isolated yield. The methylation of the triazole unit in rotaxane **2-H** followed by the anion exchange of the CH<sub>2</sub>Cl<sub>2</sub> solution with saturated NH<sub>4</sub>PF<sub>6</sub> solution can produce the target rotaxane **1-H** in a 50% yield. It should be noted that rotaxane **2-H** has only one kind of recognition site (DBA site), while rotaxane **1-H** has two kinds of recognition sites (DBA site and MTA site), as shown in Figure 2.

Rotaxanes **1-H**, **2-H** were well characterized using <sup>1</sup>H, <sup>13</sup>C NMR spectroscopy and HR-ESI mass spectrometry (Supporting Information (SI)). The 2D COSY NMR spectra of **2-H** and **1-H** were measured to assign the protons.<sup>15</sup> The reversible shuttling motion of the macrocycles between the two different recognition sites in rotaxane **1-H** was also confirmed by the <sup>1</sup>H NMR spectroscopy, as discussed below.

First, we analyzed the <sup>1</sup>H NMR spectrum of rotaxane **1-H** (Figure 3b). The comparison between the <sup>1</sup>H NMR spectra of rotaxane **1-H** and our previously synthesized rotaxane<sup>12</sup> revealed that the macrocycle **5** predominately resides around the DBA recognition station in rotaxane **1-H**.<sup>15</sup> On the other hand, compared with the <sup>1</sup>H NMR spectrum of rotaxane **2-H** (Figure 3a), there was no significant change that was observed in the peaks corresponding to the DBA recognition site in the <sup>1</sup>H NMR spectrum of [5]rotaxane **1-H**. Nevertheless, the peaks of protons H<sub>4</sub>, H<sub>5</sub>, H<sub>7</sub>, H<sub>8</sub> on or neighboring the triazole unit were shifted downfield ( $\Delta\delta = 0.45, 0.21, 0.96,$  and  $0.56$  ppm, respectively) due to the methylation of the triazole unit; meanwhile, the signal for the methyl proton H<sub>6</sub> in *N*-methyltriazolium part emerged at 4.50 ppm. The single peak of H<sub>7</sub> also confirmed the shape of rotaxane **1-H** is

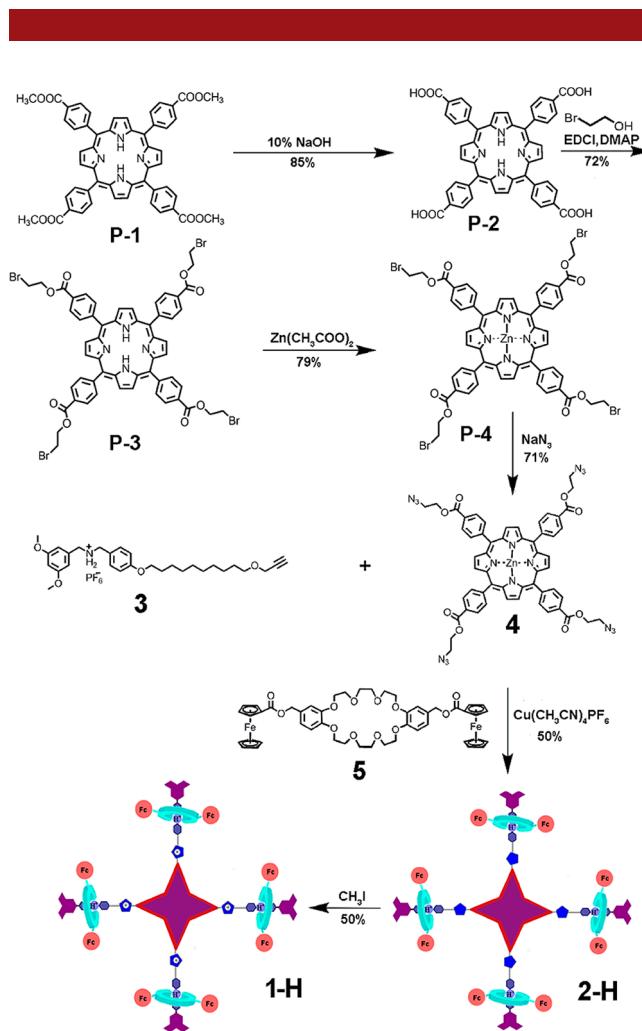


**Figure 2.** Syntheses of azide **4** and rotaxanes **2-H**, **1-H**.

symmetrical. The HR-ESI mass spectrum of the target rotaxane **1-H** (SI) also confirmed the structure as shown in Figure 1, which has the peak at  $m/z$  840.8027, corresponding to the species that lost eight PF<sub>6</sub><sup>−</sup> counterions, i.e., [M-8PF<sub>6</sub>−Zn]<sup>8+</sup>. The calculated value for rotaxane **1-H** (C<sub>368</sub>H<sub>428</sub>N<sub>20</sub>O<sub>72</sub>Fe<sub>8</sub><sup>8+</sup>) is 840.8155. The mass spectrum of rotaxane **1-H** also has the peaks emerged at  $m/z$  981.6267, 1169.4509, and 1432.2815, corresponding to the species that lost seven, six, and five PF<sub>6</sub><sup>−</sup> counterions, respectively. All this evidence confirmed that the target [5]rotaxane **1-H** was synthesized successfully as we have designed.

Next, we investigated the shuttling motion of the macrocycles between the two distinguishable recognition sites in the molecular thread of rotaxane **1-H** using <sup>1</sup>H NMR spectroscopy. After the addition of 4 equiv of 1,8-diazabicyclo[5.4.0]undec-7-ene (DBU) to the CD<sub>3</sub>COCD<sub>3</sub> solution of rotaxane **1-H**, the ammonium moiety was deprotonated; thus the DB24C8 macrocycles migrated from the DBA stations to the MTA recognition sites (Figure 1). As shown in Figure 3c, the methylene protons H<sub>14</sub> and H<sub>15</sub> in the DBA station moved upfield significantly ( $\Delta\delta = -1.01$  and  $-0.87$  ppm, respectively) because of the deprotonation and the movement of the

(14) (a) Serreli, V.; Lee, C.-F.; Kay, E. R.; Leigh, D. A. *Nature* **2007**, *445*, 523–527. (b) Silvi, S.; Arduini, A.; Pochini, A.; Secchi, A.; Tomasulo, M.; Raymo, F. M.; Baroncini, M.; Credi, A. *J. Am. Chem. Soc.* **2007**, *129*, 13378–13379. (c) Meldal, M.; Tornøe, C. W. *Chem. Rev.* **2008**, *108*, 2952–3015. (d) Trabolsi, A.; Khashab, N.; Fahrenbach, A. C.; Friedman, D. C.; Colvin, M. T.; Coti, K. K.; Benitez, D.; Tkatchouk, E.; Olsen, J.-C.; Belovich, M. E.; Carmielli, R.; Khatib, H. A.; Goddard, W. A., III; Wasielewski, M. R.; Stoddart, J. F. *Nat. Chem.* **2010**, *2*, 42–49.

(15) See Supporting Information.

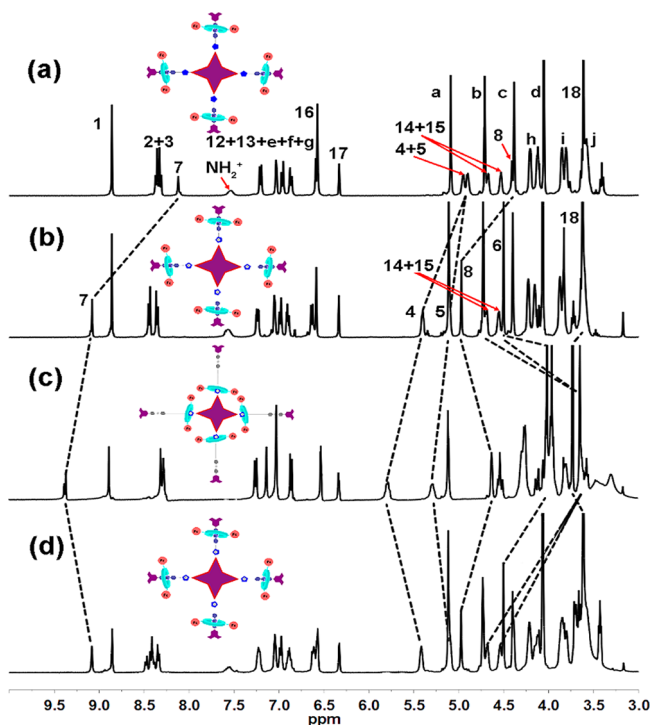


**Figure 3.** Partial  $^1\text{H}$  NMR spectra (400 MHz,  $\text{CD}_3\text{COCD}_3$ , 298 K) (a) [5]rotaxane **2-H**. (b) [5]rotaxane **1-H**. (c) deprotonation with addition of 4 equiv of DBU to sample b. (d) Reprotonation with addition of 4.1 equiv of TFA to sample c. The assignments correspond to the structures as shown in Figure 1.

macrocycles. Meanwhile, the peaks for the *N*-methyltriazolium protons were shifted due to association with the macrocyclic compound **5**, for  $\text{H}_6$  with a  $\Delta\delta$  of  $-0.54$  ppm and  $\text{H}_4$ ,  $\text{H}_5$ ,  $\text{H}_7$ , and  $\text{H}_8$  with  $\Delta\delta$  of 0.37, 0.19, 0.31, and  $-0.36$  ppm, respectively. All these observations indicated that the DB24C8 macrocycles moved to the MTA recognition sites. The 2D NOESY NMR spectrum of **1-H** after the addition of DBU also confirmed the location.<sup>15</sup> The  $^1\text{H}$  NMR spectrum was completely recovered after the reprotonation of the  $-\text{NH}-$  center with the addition of 4.1 equiv of  $\text{CF}_3\text{CO}_2\text{H}$  (TFA) (Figure 3d), indicating the return of the DB24C8 rings to the DBA stations. Thus, by  $^1\text{H}$  NMR spectroscopic measurements, the acid–base

(16) (a) Mateo-Alonso, A.; Ehli, C.; Rahman, G. M. A.; Guldi, D. M.; Fioravanti, G.; Marcaccio, M.; Paolucci, F.; Prato, M. *Angew. Chem., Int. Ed.* **2007**, *46*, 3521–3525. (b) Mateo-Alonso, A.; Guldi, D. M.; Paolucci, F.; Prato, M. *Angew. Chem., Int. Ed.* **2007**, *46*, 8120–8126. (c) Mateo-Alonso, A.; Iliopoulos, K.; Couris, S.; Prato, M. *J. Am. Chem. Soc.* **2008**, *130*, 1534–1535. (d) Mateo-Alonso, A.; Ehli, C.; Guldi, D. M.; Prato, M. *J. Am. Chem. Soc.* **2008**, *130*, 14938–14939. (e) Mateo-Alonso, A.; Prato, M. *Eur. J. Org. Chem.* **2010**, 1324–1332. (f) Scarel, F.; Valenti, G.; Gaikwad, S.; Marcaccio, M.; Paolucci, F.; Mateo-Alonso, A. *Chem.—Eur. J.* **2012**, *18*, 14063–14068.

induced reversible shuttling motion of the macrocycles along the rotaxane thread in [5]rotaxane **1-H** has been demonstrated. In addition, from the spectra, it can be concluded that the movement of four macrocycles is simultaneous.

Finally, the photophysical properties of rotaxane **1-H** were also investigated.<sup>15</sup> In our previous work,<sup>12b,c</sup> we have demonstrated that the movement of the ferrocene-functionalized macrocycle<sup>16</sup> can result in a dramatic decrease in fluorescence intensity of the fluorophore. However, in this system, the fluorescence intensity of the porphyrin increased. This weird phenomenon may be explained by the fact that the zinc porphyrin core can coordinate with the nitrogen atoms on the DBU molecule. To confirm this explanation, DBU was added to the solution of zinc tetraphenylporphyrin (**zinc-TPP**), the fluorescence intensity of **zinc-TPP** was observed to also increase (Figure S3).

In summary, a novel star-shaped zinc porphyrin cored [5]rotaxane, with four DB24C8 macrocycles interlocked onto the thread component containing a zinc porphyrin core was synthesized and well characterized. The simultaneous shuttling motion of the macrocycles between the DBA station and the MTA station can be driven by external acid–base stimuli. By introducing a zinc porphyrin core into the center of the rotaxane, the shape of the rotaxane becomes very symmetrical. This kind of porphyrinic rotaxane with a highly symmetrical geometry exhibits important potential for the construction of large sophisticated assemblies. Most importantly, the synthetic principle described in this paper should be generalized so as to synthesize more complicated rotaxanes in the future.

**Acknowledgment.** We thank the NSFC/China (20902024, 21272073, and 21190033), the National Basic Research 973 Program (2011CB808400), the Foundation for the Author of National Excellent Doctoral Dissertation of China (200957), the Fok Ying Tong Education Foundation (121069), the Fundamental Research Funds for the Central Universities, and the Innovation Program of Shanghai Municipal Education Commission for financial support.

**Supporting Information Available.** Experimental procedures and characterizations for all intermediates and compounds;  $^1\text{H}$ ,  $^{13}\text{C}$  NMR spectra; HR-ESI mass spectra of all compounds; 2D COSY and NOESY NMR spectra of **2-H** and **1-H**; UV–vis absorption spectra; fluorescence spectra of compounds **1-H** and **zinc-TPP**. This material is available free of charge via the Internet at <http://pubs.acs.org>.

The authors declare no competing financial interest.